Heliyon 9 (2023) e17145

Contents lists available at ScienceDirect

Heliyon

journal homepage: www.cell.com/heliyon

Impact of Internal CFRP strips on the flexural behavior of heat-damaged reinforced concrete beams

Rajai Z. Al-Rousan

Civil Engineering Department, Jordan University of Science and Technology, Jordan

ARTICLE INFO

Keywords:
Elevated temperature
Internal CFRP Strips
Reinforced concrete beams
Flexural
Carbon fiber

ABSTRACT

Recent theoretical developments revealed that reinforced concrete (RC) structures are susceptible to deterioration risk upon exposure to high temperatures where the mechanical properties of their constituents are affected and therefore require upgrading their overall performance. However, the overall behavior could be improved by strengthing the RC beams using the well-known carbon fiber-reinforcement polymers (CFRP) materials where its efficiency is highly limited by detachment, and debonding problems appear as a result of the weakness in the bond between the concrete surface and the strengthening material or upon the stress concentration induced by the various anchoring systems. The CFRP sheets have been integrated as internal reinforcement in the maximum bending zone within the thermally damaged beams, a new technology used in this study. The suggested method was the first of its kind and did not need an adhesive to be applied where debonding problem is eliminated. In contrast to conventionally reinforced steel, CFRP composite materials are fully compatible with flexural steel and constrained concrete. A total of 40 RC with (150 × 200) mm^2 and an overall length of 1100 mm concrete beams were cast, and the studied parameters were the CFRP length, position, and exposure temperature. The internal strengthening technique has been found to ensure the full utilization of the strengthening material where the externally-strengthened beams fail preceding the CFRP strain reached, and this was confirmed using the linear weighted sum method where the internal strengthening has the highest ranking based on the mechanical characteristics comparisons. Moreover, the internal CFRP reinforcement improves RC beam performance, strength, stiffness, toughness, and serviceability more than exterior CFRP sheets. However, the enhancement percentages are twice as much for internal strengthening as the external one. It has also been found that the reinforcement's location substantially impacted the number and length of flexural cracks and its failure mode. In addition, for every 1% reduction in concrete compressive strength in heat damage, the average ultimate load was reduced by 0.8%. The CFRP profitability indexes decrease as sheet number and temperature increase; the average toughness decrease at 150 °C, 250 °C, and 500 °C is 12%, 21%, and 47%, respectively.

1. Introduction and literature review

RC is the commonly utilized building material because of its simplicity, strength, and ability to modify its capabilities by combining it with different additives. According to environmental exposure and loading conditions, RC structures deteriorate over time, which

E-mail address: rzalrousan@just.edu.jo.

https://doi.org/10.1016/j.heliyon.2023.e17145
Received 21 September 2022; Received in revised form 26 May 2023; Accepted 8 June 2023
Available online 9 June 2023

may change how they perform and the stresses they can sustain, and this might be caused by creating an opening within the different structural elements [1,2]. Moreover, in the case of elevated temperature exposure, the resulting deterioration affects the overall mechanical properties of concrete and steel materials, such as compressive and tensile strength. It has been realized that the extent of degradation is highly limited to the exposed temperature level where a significant degradation appears at temperatures higher than 500 °C. Due to their exceptional characteristics in terms of high strength-to-weight ratio, corrosion resistance, and ease of application, carbon fiber reinforced polymer (CFRP) composites have emerged as an attractive and dominant technology for reinforcing and repairing RC structures for normal [3,4] and lightweight concrete [5]. This paper represents a relatively new field that has emerged from studying reinforced concrete behaviors. Carbon fiber-reinforcement polymer (CFRP) composites are used for all structural purposes, including strengthening and repairing existing deficient reinforced concrete (RC) structures. Concrete beams can be repaired or strengthened with CFRP to improve shear and flexure performance. According to the empirical hypotheses, delamination between the CFRP composites and the concrete is a common failure mode for RC beams that have been externally reinforced with CFRP composites [6]. Moreover, Al-Osta et al. [7] stated that providing CFRP sheets into RC beams increases their ultimate strength and stiffness capabilities, especially if well-anchored.

Composite materials (CFRP) have recently emerged as one of the most promising composite materials and systems for strengthening and retrofitting structures [8]. However, CFRP has higher tensile strength than other FRP types and traditionally-used steel material. Recent studies show that its strength is not fully utilized due to brittle tensile behavior, debonding problem, and the general persuade, which enhances the ultimate loads of the repaired or strengthened RC specimens [9]. However, the performance of the utilized material is significantly affected by the bond strength at the concrete interface [10,11], which could be addressed by the Response Surface Methodology (RSM) [12]. The debonding problem is mainly related to the externally bonded sheets or plates [13]. Externally-bonded composites made of CFRP material have been utilized as additional external reinforcement in shear and flexure to strengthen and repair RC structures in which the construction method impacts performance and durability [14]. However, according to investigations, structures reinforced with CFRP are vulnerable to debonding failure, in which the CFRP material separates from the concrete during the initial phases of loading, and it could be reduced by utilizing bonding agents with high strength, especially when concrete loses its mechanical characteristics under being exposed to high temperatures [15]. The CFRP strips resist acid, alkali, and organic solvents since they do not absorb moisture. As a result, they do not significantly deteriorate in moist, salty conditions or in freezing climates where salts are needed to melt ice. Hence, it is acknowledged that CFRP strips are the most advantageous material to use instead of traditional steel stirrups in RC beams for shear strengthening or could be combined with conventional steel reinforcement for flexural strengthening [16].

The bond strength between the concrete surface and CFRP composites, restricted by the adhesive material's qualities used to link the CFRP composites with the concrete, is a dominant problem in their external application. Due to debonding issues caused by this restriction, CFRP composites are not profitable to their full potential. As a result, anchorage systems are employed to strengthen the link between the concrete surface and CFRP composites, increasing RC beam's flexural and shear strength [17–19]. However, the efficiency of utilizing CFRP for retrofitting heat-damaged RC beams was examined by Al-Abdwais et al. [20], where it has been realized that enhancing the properties of bonding material used in external CFRP strengthening resulted in increasing the strengthening material contribution.

Currently, the CFRP material is frequently utilized to repair and strengthen composite materials of RC structures with flexure or shear deficiencies. That is because the CFRP increases concrete structures' shear or flexural capacity when utilized to strengthen them externally. This composite material's ability to transfer stress from the concrete debonding surface to the CFRP composite components and maintain structural integrity depends on the bond condition. The success of externally reinforcing weak RC members depends on the strength of the bond between the concrete surface and the CFRP composite materials. Several experimental studies have confirmed that externally-bonded CFRP composites significantly improved RC elements' flexure and shear strength [21–23]. Even when using the adhesive material recommended by the manufacturers, the debonding problem still exists, particularly in highly stressed areas or around the composite's ends. When an abnormal load occurs, or one of the main structural elements is removed due to a change in the structure's purpose, overloading and redistributing the original design loads occur. As a result, it must be strengthened to compensate for its lack of flexure or shear. To achieve a ductile failure mode, flexural and shear strengthening must be performed simultaneously [24,25].

Because of increasing temperatures, RC constructions, particularly beams, are vulnerable to deformation or fracture. In fact, the RC beams lose their stiffness and strength as a result of the high temperatures [26]. The high temperatures also affect the mechanical properties of steel rebar and concrete, which respond to how the beam's stresses are distributed [26,27]. Findings demonstrate that exterior-bonded CFRP sheets and laminates improved heat-damaged beams' flexural capacity and shear behavior. Studies have shown that bonding CFRP materials to the external concrete surface enhances the structural shear performance. Moreover, research has demonstrated that this reinforcement helps heat-damaged structures partially restore their flexural strength. It is essential to point out that the quality of a substance in terms of either structural recovery or strengthening is determined by several different factors, some of which are as follows: resistance to very high temperatures, the type of the fiber used, type of analysis, resistance to energy integrity, the anchoring system, heating condition, the damage degree, and the safety factors of bridges strengthened with CFRP [28,29].

The repetitive heating-cooling cycles in the extremely risky location exposed to heat actions significantly impact the structural stability and integrity. So, when analyzing and designing these structures, these cycle effects must be considered [30,31]. It should be mentioned that as long as the temperature is below 300 °C, structural concrete maintains its mechanical properties. As the temperature exceeds 500 °C, the properties of the concrete, however, deteriorate. Due to the significant temperature difference between the surface and core of the concrete, its characteristics are significantly affected when exposed to fire.

The cement paste and aggregates expand and contract due to the temperature difference, generating tensile strains on the con-

crete's surface and resulting in material cracking. Several factors determine the severity of the damage to the concrete elements. Examples of these variables include the size of the structure, the cement and aggregates used, the amount of moisture in the concrete, the length of time and rate of exposure to excessive heat, the cooling mechanism chosen, and the maximum temperature [32]. The CFRP materials are featured because they are durable, easy to transport and install, and extremely strong due to a high strength-to-weight ratio, excelling the reinforced-by-steel structures, which mostly collapse when exposed to dynamic loads and corrosion [33]. Moreover, a hybrid system (CFRP composites with conventional steel reinforcement) is recently used and offered a sufficient opportunity to develop high-performance and economic structures [34]. However, the heat-damage condition might occur after the strengthening material is applied, and it could be protected using various techniques. One approach is done using the facle method utilized in the research of Wang et al. [35], where nanosheets β-FEOOH particles are applied using the double-layered hydroxide (DLH) technique, resulting in improving the thermal stability and the resistance of the epoxy adhesive. Moreover, a second approach for improving the fire safety of epoxy resin was used by Wang et al. [36] in another research in 2017, where a layer-by-layer method was utilized on the solid surface of TiO_2 spheres by the zinc hydroxy stannate (ZHS).

The hybrid and optimal use of different construction materials has emerged as a very promising direction in structural engineering for developing economic and high-performance structures, which are especially desirable in rapidly urbanizing countries. To increase the effectiveness of the CFRP composite strengthening/repair technique in construction, it is necessary to have a logical understanding of the response of strengthened members. As a result, this research examined the feasibility of using CFRP composite strips as internal reinforcement or additional flexural reinforcement in RC beams. This study aims to eliminate the debonding mode of failure and anchoring technique because no epoxy is needed and to relieve potentially congested longitudinal steel reinforcement bars.

Using CFRP sheets as internal reinforcement is a simple strengthening technique that does not require any adherence procedures because they are confined by concrete material, which plays an important role in connecting the beam's components (concrete, steel, and CFRP). Meanwhile, the method of internal strengthening could be used in a variety of situations, including the high flexural force, repairing or strengthening any damaged or warned structures against fire attacks, and serving as the primary reinforcement during beam casting, particularly in areas of steel congestion such as beam-column joints. In contrast, there is some limitation to utilizing the proposed techniques, mainly applied only before concrete casting. Therefore, high attention is required for the strengthening material to remain in its position. Besides, the internal strengthening technique is limited in its use for RC members before being casted or repaired after the concrete cover is replaced. The study in hand assesses the probability and feasibility of utilizing a new strengthening technique where the main aim is to remove the unfavorable debonding problems of the CFRP sheets usually occur in the external strengthening approach and the induced difficulties in the anchoring systems. Therefore, the newly proposed technique helps increase the feasibility and performance of the strengthening system since there is no need to use an epoxy adhesive material which is the main source of the debonding issue that worsens under the effect of high temperatures. As a result, the source of debonding-the adhesives-is absent, which minimizes the overflow and the peal of strips post and before exposure to high temperatures. This study adopted an exploratory approach to determine the enhancement in flexural and ductility behavior of defective RC beams reinforced internally using CFRP sheets. These CFRP strips are (400 mm, 600 mm, and 800 mm) in long elevated temperatures (23 °C, 150 °C, 250 °C, and 500 °C).

2. Methodology

The methodology section is mainly divided into main sections. The first one is the material subsection, describing the different used materials (concrete, steel, CFRP strips, and epoxy adhesive). The second is the methods subsection, which describes the specimen molding, CFRP strengthening, and heat treatment procedures.

2.1. Materials

Concrete material was designed per the ACI [37] design procedure, which required tap water, category I normal Portland cement, crushed fine aggregate, and crushed coarse aggregate to ensure concrete uniformity in all tested beams [38]. The Portland cement (OPC) chemically consists of tri and dicalcium silicates, tricalcium aluminate, tetracalcium alumino ferrite, and calcium sulfate as gypsum. In the presence of water, it can bind mineral particles together owing to its adhesive and cohesive characteristics, creating a continuous, compact mortar mass. However, the physical properties of the utilized cement are illustrated in Table 1. Moreover, the gradation of the coarse and fine aggregates is provided in Fig. 1(a) and Fig. 1(b), respectively. Concrete was designed to achieve a 50 MPa in compressive strength (ASTM C579 standard, method B [39]) and 4.31 MPa in tensile (ASTM C496 standard [40])at a room

Table 1
Physical properties of ordinary Portland cement.

Properties	Quantity
Specific gravity	3.15
Normal consistency (%)	28
Initial setting time (min)	63
Final setting time (min)	274
Fineness (kg/m^2)	328
Bulk density (kg/m^3)	850

temperature of 23 °C with 80 mm slump value (ASTM C143/C143 M [41]), and the mixing components proportions are shown in Table 2. Moreover, steel bars of Grade 60 were used with a yield strength value of 60 MPa.

The strengthening material comprises two main parts; CFRP strips and epoxy adhesin provided by SIKA company with the following names (SikaWrap® −300 °C) and (Sikadur®-330). Firstly, concrete surfaces were painted with Sikadur® −330 epoxy (resin and hardener parts) in 4:1 proportions, which were mixed with a mechanical drill for (3–5) minutes to get the appropriate consistency [42]. The plies were then put on the painted beams. Table 3 displays the sheets' and epoxy's mechanical and physical properties. Furthermore, the mechanical properties of the materials used, such as concrete, steel, epoxy, and CFRP material, are predicted to deteriorate after being subjected to high temperatures. The consequent deterioration in concrete material has been addressed in compression and tension, where concrete cylinders were casted and subjected to various testing temperatures before being evaluated for mechanical characteristics.

2.2. Methods

2.2.1. Specimens description

Fourty Reinforced Concrete beams have been casted with a width of 150 mm and depth of 200 mm, respectively, with an overall length of 1100 mm. Beams were simply supported, having one end with roller support restricting the movement in the vertical direction and the other a hinge support with the movement restricted in the vertical and horizontal directions. The RC beams have been tested under the four-point testing procedure, as illustrated in Fig. 2. Main flexural reinforcement was provided in the tension and compression regions of the beam with two steel bars of 10 mm diameter each, and shear reinforcement was provided in forms of stirrups spaced 50 mm along the 300 mm from the first one placed on both sides within the maximum shear regions, besides the middle 400 mm left without shear reinforcement since there is no shear action at the maximum bending moment region. Beams were strengthened using CFRP composites of 50 mm strip width and three different length values (400, 600, and 800) mm positioned at the bottom face of the beam, as shown in Fig. 3 (a-c). However, length values were chosen to examine the effective development length that ensures the highest benefit from utilizing the CFRP composite, where 400 mm was provided to cover the maximum moment region. The other values examined the efficiency of extending the strengthening material outside the loading points.

The details of the tested specimens are illustrated in Table 4, where four main parameters were studied; CFRP strengthening (strengthened and un-strengthened), four temperature values (23 °C, 150 °C, 250 °C, and 500 °C), three CFRP strips lengths (400, 600, and 800) mm, and two reinforcement positions (external and internal). However, a beam with the following designation (FB1T23-400-E) demonstrates that the tested beam is from the first set (strengthened) with an external CFRP strip of 400 mm length and tested at room temperature (23 °C).

2.2.2. Mixing and thermal treatment procedures

Concrete components were mixed using the 0.15 m^3 capacity tilting drum. Firstly, the internal surface of the mixer was witted with the required amount of crushed concrete aggregate being added. This is followed by the addition of the remaining components gradually, including the cement, water, and fine aggregate, besides adding some superplasticizer to enhance the mixture's workability without any excess amount of water. The mixture was left for 5 min inside the mixer after the mixing was done to set up, then it was poured into 150 × 200 × 1100 mm^3 wooden molds and compacted by an electronic vibrator, as shown in Fig. 4 (a-g). The beam specimens were left for 24 h before being de-molded. After that, they were treated in a pool of lime-saturated water for 28 days.

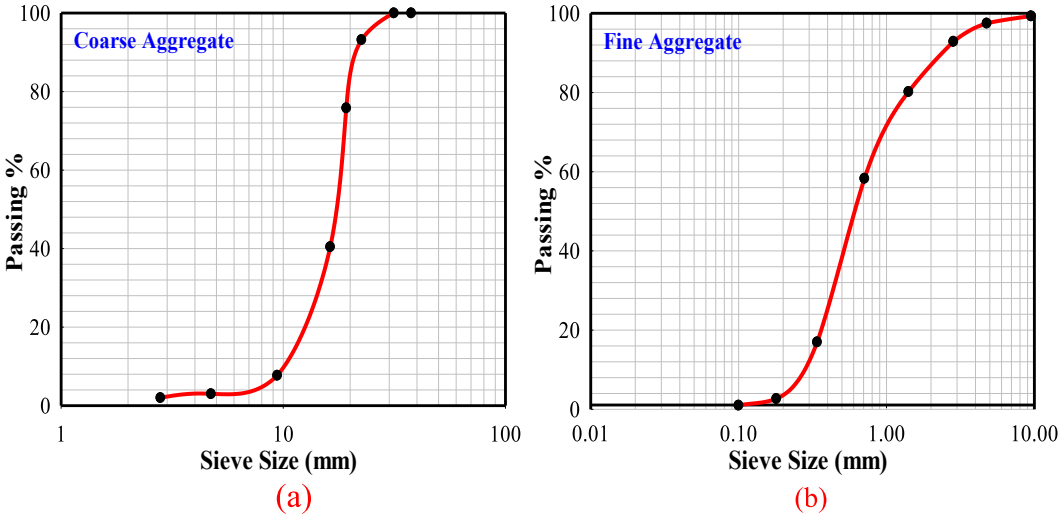

Fig. 1. Aggregate grading curves (a) Coarse aggregate, and (b) Fine aggregate.

Table 2
Mixture proportions of concrete.

Material	Proportions (kg/m^3)
Cement	422
Fine Aggregate	621
Coarse Aggregate	706
Water	147.6
Superplasticizer	As required

Table 3
Physical and mechanical properties of Sika epoxy and CFRP sheet.

Sika Epoxy	Tensile Strength	30 N/mm^2
	Break Elongation	0.9%
	E-Modulus	Flexural: 3800 N/mm^2 Tensile: 4500 N/mm
Sika CFRP Sheet	Fabric Thickness	0.167 mm
	Elongation break	1.67%
	Tensile Strength	4000 N/mm^2
	Tensile Modulus	230,000 N/mm^2

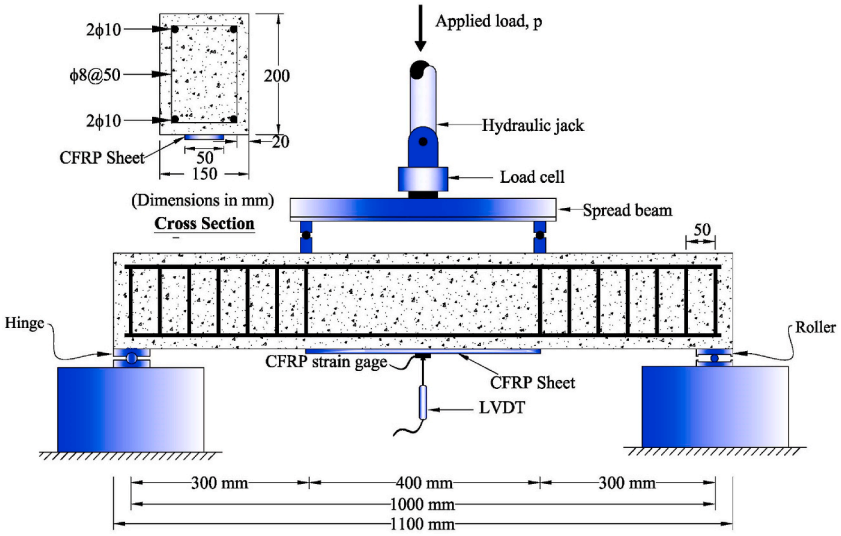

Fig. 2. Beams reinforcement, dimensions, instrumentations, and test setup.

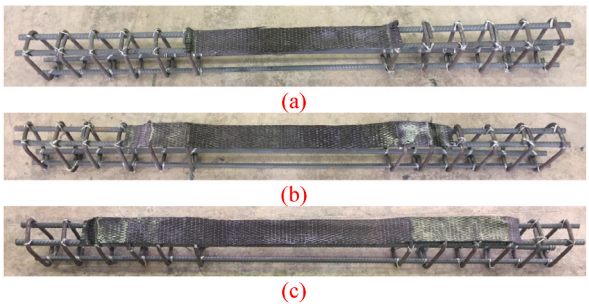

Fig. 3. CFRP strips internal attachment (strip width = 50 mm) with different CFRP lengths (a) 400 mm, (b) 600 mm, and (c) 800 mm.

Table 4
The details and results tested flexural beams.

Group	Specimen	T, °C	Strengthening Position	CFRP Length, mm	P_u, kN	Δ_u, mm	ε_{CFRP}	$\varepsilon_{CFRP}/\varepsilon_{fu}$ (%)
1	FB1T23-0-E	23	External	None	114.5	12.5	–	–
	FB1T23-400-E			400	130.7	14.1	5179	31
	FB1T23-600-E			600	140.5	14.9	5965	36
	FB1T23-800-E			800	156.6	16.0	6995	42
2	FB2T23-0-I	23	Internal	None	114.5	12.5	–	–
	FB2T23-400-I			400	139.0	15.3	6907	41
	FB2T23-600-I			600	169.2	17.9	9041	54
	FB2T23-800-I			800	202.1	20.8	12042	72
3	FB3T150-0-I	150		None	93.1	11.8	–	–
	FB3T150-400-I			400	109.9	13.2	5676	34
	FB3T150-600-I			600	134.4	14.7	7141	43
	FB3T150-800-I			800	166.3	17.0	8918	53
4	FB4T250-0-I	250		None	76.4	11.1	–	–
	FB4T250-400-I			400	91.2	12.1	4171	25
	FB4T250-600-I			600	110.2	13.3	5596	34
	FB4T250-800-I			800	135.8	15.8	7278	44
5	FB5T500-0-I	500		None	55.8	10.8	–	–
	FB5T500-400-I			400	70.7	11.4	3643	22
	FB5T500-600-I			600	87.1	12.0	5036	30
	FB5T500-800-I			800	103.6	12.8	6122	37

Note: P_u: Load at ultimate, Δ_u: Deflection at ultimate, T: Temperature, ε_{CFRP} is the CFRP strain and ε_{fu} is the CFRP ultimate strain of 16700 με.

However, for the thermal treatment process, samples were placed in the furnace for 2 h to be heated to 150–500 °C degrees. Following that, they were allowed to cool in the oven. Temperature and exposure duration were regulated by an automatically controlled electrical furnace (Fig. 5). (Maximum temperature of 1200 °C).

2.2.3. *CFRP strengthening*

After the beam specimens had been removed from the wooden molds, the externally strengthened specimens where their bottom surface was roughened and scraped using a steel wire cup brush while covered by plastering tape to prevent the rest of the area from being filled with epoxy, as shown in Fig. 6 (a, b). The bonded region was then carefully cleaned with a vacuum cleaner before cutting and preparing a 50 mm wide by 200 mm long CFRP strip. The epoxy components (parts A and B) were gently mixed for at least 3 min with a low-speed electric drill to achieve homogeneity. The cutted CFRP strip has been glued with epoxy at the top of the bonded region. However, the air bubbles were removed from the bonded CFRP strip by rolling it with a plastic roller. Finally, another layer of epoxy is put and distributed (ASTM C1583 standard [43]). However, for internal strengthening specimens, the CFRP strips were placed in their positions before pouring the concrete into the wooden molds carefully without needing any adherence material where it takes

Fig. 4. Preparing of reinforced concrete beams (a) Mixture ingredients preparation, (b) Tilting drum mixer, (c) Wooden mold, (d) Vibrator compacting, (e) Concrete casting, (f) Cylinders casting, and (g) Beams curing for 28 days.

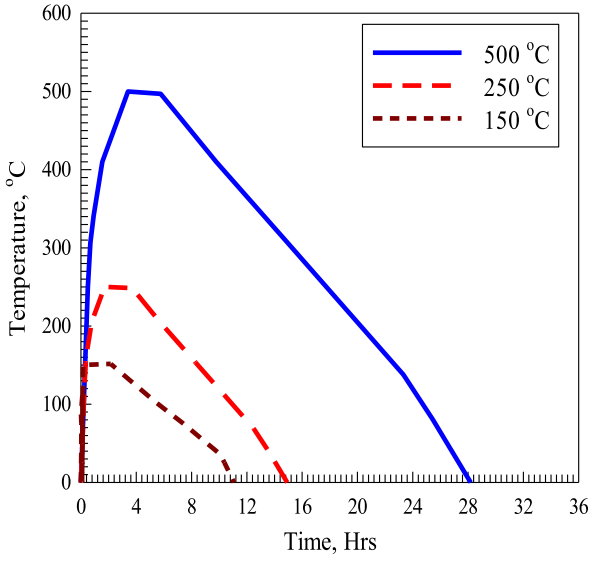

Fig. 5. The time-temperature schedule.

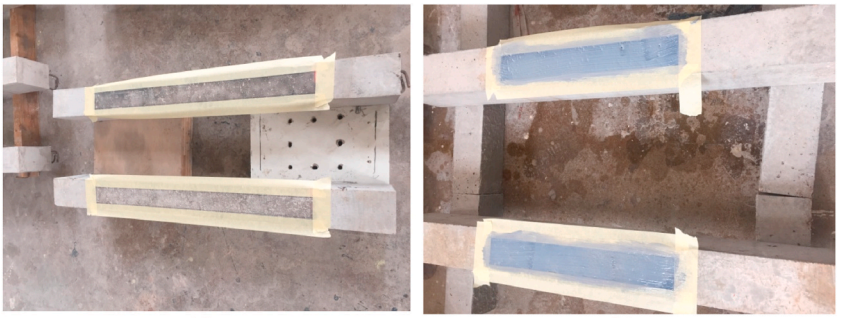

Fig. 6. Bonding of external CFRP sheets (Group #1) (a) Roughing and cleaning the surface of beam and then Marking the area of CFRP sheets bonded using plastering tape, and (b) Applying the two layers of epoxy onto CFRP sheets surface.

place inside the hardened concrete.

2.2.4. *Test equipments*

Beams were tested under a four-point testing procedure with simply-supported boundary conditions, as shown in Fig. 2. However, loading was applied using a specialized actuator calibrated using a loading cell. Besides, testing data were collected using a specialized data collecting system for servo controlling along with the global system software of the ATLAS data acquisition (DAQ) system during the experiment. Moreover, deflection values were recorded accurately at the beam mid-span using a "linear variable displacement transducer" (LVDT). Testing has been done under a 0.5 kN/s loading rate. Finally, CFRP strip strain readings were recorded using a pair of strain gauges positioned at the center of each utilized strip.

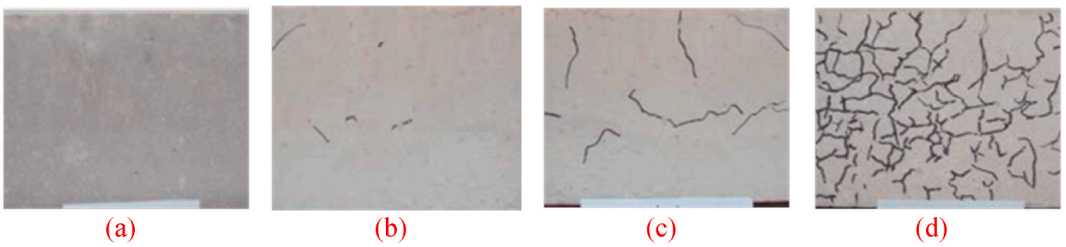

Fig. 7. Crack patterns in concrete samples (150 × 150 × 200) exposed to elevated temperatures (a) 23 °C, (b) 150 °C, (c) 250 °C, and (d) 500 °C.

3. Results and discussion

3.1. Cracking intensity and severity

In order to evaluate the effect of temperature on the beam's surface, Fig. 7 (a-d) shows (150 × 150 × 200) concrete samples cracking after being exposed to temperatures of 23 °C, 150 °C, 250 °C, and 500 °C. It has been observed that the sample's surfaces exposed to a temperature of 250 °C had just a few cracks. Also, it has been revealed that a temperature increase worsens the number and size of cracks. When the samples are subjected to 150 °C, the cracks diminish; however, they intensify when exposed to 500 °C. Due to thermal damage, cracks developed in the shape of a spider web. Nonetheless, it is generally known that concrete surfaces exposed to high temperatures start to crack, which intensifies and spreads as the temperature increases. The propagation of additional stress and the delaying of the projected hydration in the concrete components, which lowers the specified concrete compressive strength, are significantly influenced by variations between the cement paste and aggregate expansion coefficient. As observed in Fig. 8(a), the crack intensity was measured computationally using high-quality images by AutoCAD software. However, the cracking intensity and width could increase when the exposed temperature approaches 250 °C without being affected below this level. Whenever temperatures exceed 200 °C, the expansion rate is 2.5 per 50 °C for cracking severity and 0.015 mm per 50 °C for crack width (Fig. 8(b)).

3.2. The effect of heat damage on concrete strength and failure modes

The mechanical properties of concrete and steel materials are affected by various degrees depending on the exposure temperature. However, concrete material is significantly affected by high temperatures over 100 ° C, and its degradation extent increases rapidly, including its elastic modulus, compressive, and tensile strength capacities. Upon continuous heating, concrete moisture evaporates, and the temperature inside the RC beams increases, causing the degradation of its constituents [44]. Based on the literature, a reduction factor k_c was proposed by the Eurocode [45], as illustrated in equation (1) and Fig. 9(a). In addition, it has been realized that the steel reinforcement is minorly affected by temperatures less than 600 ° C.

$$k_c = \begin{cases} 1 & T \le 100 \\ 1.067 - 0.00067T & 100 \le T \le 400 \\ 1.44 - 10.16T & 400 \le T \le 900 \\ 0 & 900 \le T \end{cases} \quad (1)$$

Fig. 9(a and b) concisely illustrates how elevated temperatures affected the RC specimens and shows the residual temperature vs. compressive and tensile strength curves. The figures demonstrate that the splitting and compressive strength significantly decreased at temperatures above 250 °C, whereas the reduction was minimal at 150 °C. This outcome may be attributed to thermally induced cracks, the weakening of the cement paste ingredients at high temperatures, or both. The intense and concentrated concrete cracking that develops due to the heating scenario is known as map cracking, and it gets more severe as the temperature increases with no visible surface difference. According to Fig. 9(b), the residual strengths (compressive and splitting) decreased from 91% to 89% at 150 °C to 45% and 43% at 500 °C, respectively.

The crack's development was monitored during the flexural testing of the strengthened and heat-damaged RC beams, as appeared in Fig. 10(a–d) and Fig. 11(a and b), for the unstrengthened and strengthened beam groups, respectively. Observing the cracking failures appeared in Fig. 10 (a, b) for the heat-damaged un-strengthened RC beams where the flexural failure was recorded for all tested specimens. Flexural cracks appear within the maximum bending moment region at the middle of the beam, especially between the two

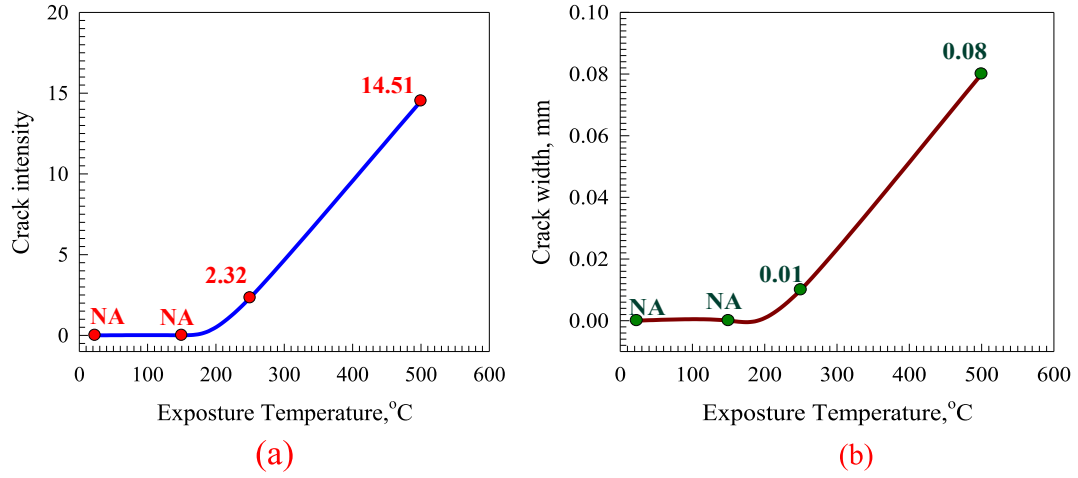

Fig. 8. (a) Crack intensity and (b) crack width in concrete.

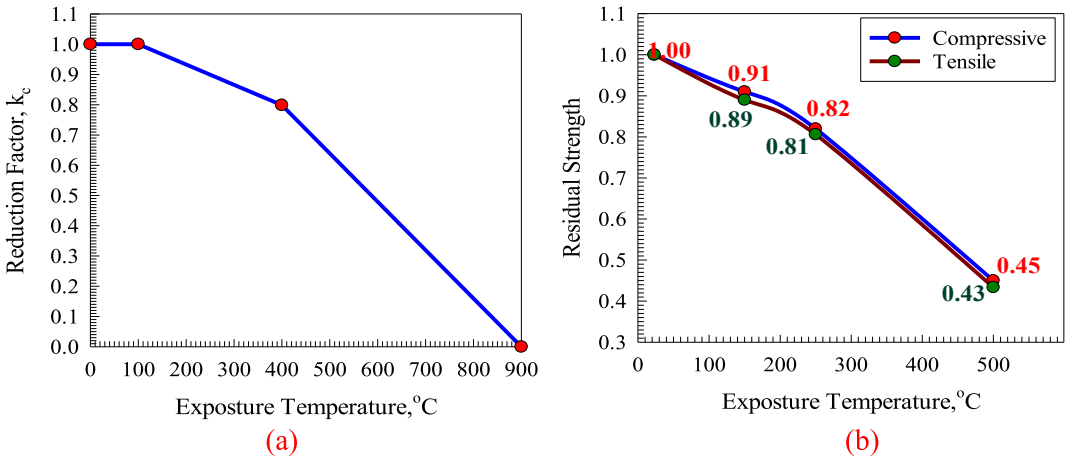

Fig. 9. Compressive and splitting strengths residuals (a) Eurocode [45], and (b) Experimental.

loading points. Cracks initiate firstly at the middle span, followed by the development of more flexural cracks to the right and left of the firstly developed crack. However, flexural cracks become more intense in their number and more severe under higher exposed temperatures where the mechanical properties of concrete material were reduced, and the resulting reduction increased under increasing the tested temperatures. This is also accompanied by a probability of concrete crushing between the two loading points. For heat-damaged specimens, the cracks' length increased and expanded from the bottom of the beam toward their top fiber.

The failure modes of the second tested RC beams are illustrated in Fig. 11 (a, b). It has been found that the length of the CFRP sheet affects the size, distribution, and length of visible cracks. In addition, it has been shown that when the temperature and length of the CFRP sheet increased, the distribution and number of flexural cracks increased as well. This phenomenon typically occurs because CFRP sheets have the potential to heal cracks by providing enough development length. Also, as shown in Fig. 11 (a, b), the location of the reinforcement (internally or externally) had a substantial impact on the number and length of flexural cracks. However, it has been demonstrated by Barris et al. [8] that strengthening the RC beams internally or externally using the NSM technique might cause the failure mode to be changed based on the amount of flexural reinforcement provided.

In contrast to external strengthening, the level of damage has been demonstrated to be greater for internal reinforcing. The resulting cracking restriction may make sense in the case of internal strengthening. It must be kept in mind that the length effectiveness of the CFRP sheet enhances the structural flexural capacity that causes that represents the major cause for the concrete crushing in the middle of the beam. Internally reinforced CFRP beams might be subjected to various cracking at multiple locations due to the considerable CFRP development length provided within the RC beam. As seen in Fig. 11 (a, b), this behavior may subject the building vulnerable to a potential CFRP sheet rupture. In contrast, beams strengthened with external CFRP failed in bending, and delamination at the end strip location was induced and could be mitigated by providing proper anchoring [46,47]. That happened because the interfacial adhesion strength exceeded the ultimate tensile stress levels permitted by the material. Nonetheless, the beam's internal core suffered minor flexural cracks compared to the control beam.

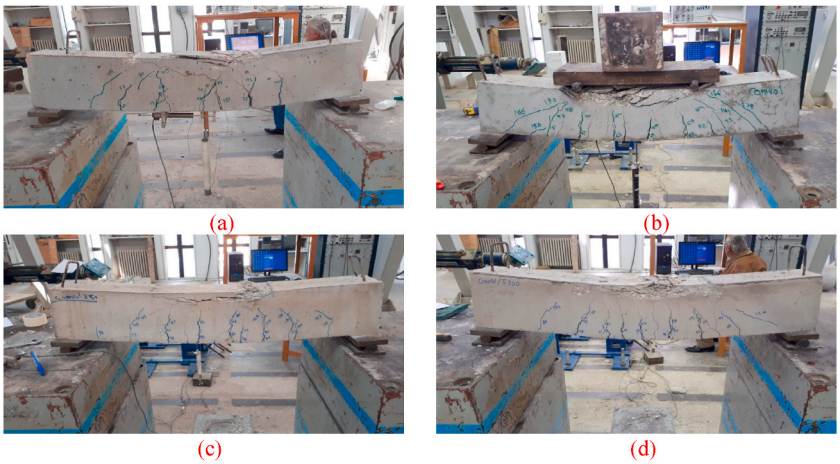

Fig. 10. The impact of temperature on the mode of failure of control beams (a) 23 °C, (b) 150 °C, (c) 250 °C, and (d) 500 °C.

Fig. 11. The impact of strengthening technique on the mode of failure of (a) Internal strengthening, and (b) External strengthening.

3.3. CFRP tensile strain, ultimate loading, and ultimate deflection

The ultimate load and its accompanied deflection values are normalized with respect to the control beam and figured out in Table 4 and Fig. 12 (a, b). The ultimate strength of externally strengthened beams was increased by 14%, 23%, and 37%, respectively, using CFRP lengths of 400 mm, 600 mm, and 800 mm, whereas the maximum deflection increased correspondingly by 13%, 19%, and 28% and it was approximately 74% of the improvement recorded in the ultimate strength capacity. Integration of the CFRP lengths of (400 mm, 600 mm, and 800 mm) increased the ultimate strength of the beams internally reinforced with CFRP sheet by 21%, 48%, and 77%, respectively. This equals 1.97 times the enhancement percentages observed in the exterior CFRP technique. The results of Jafarzadeh and Nematzadeh [48] showed that flexural strengthening using CFRP sheets improved the flexural capacity of the specimens, and this performance improvement became more notable with an increase in the exposure temperature.

According to Fig. 12(b), the corresponding enhancements in ultimate deflection values were 23%, 44%, and 66%, corresponding to 2.21 times the enhancement percentages recorded in the external CFRP methodology. The main findings of this study suggest that applying a CFRP sheet as internal strengthening instead of an external one has a higher effect on the flexural strength of RC beams. Applying one 400 mm-long CFRP sheet for internal strengthening is preferable over employing the identical length CFRP sheet for external strengthening since the exterior strengthening was not as effective as the interior one regarding ultimate load among all scenarios. However, it has been revealed by Ref. [49] that increasing the number of utilized FRP sheets increased the overall performance of the beam, especially the load-carrying capacity.

According to Fig. 12(a), the average failure load for beams subjected to 150°, 250°, and 500 °C decreases by 6%, 9%, and 29%, respectively, compared to control beams at ambient temperatures. Also, for elevated temperatures of 150 °C, 250 °C, and 500 °C, a reduction in concrete's compressive strength of 9%, 18%, and 55% resulted in decreases in ultimate load by 19%, 34%, and 49%. These

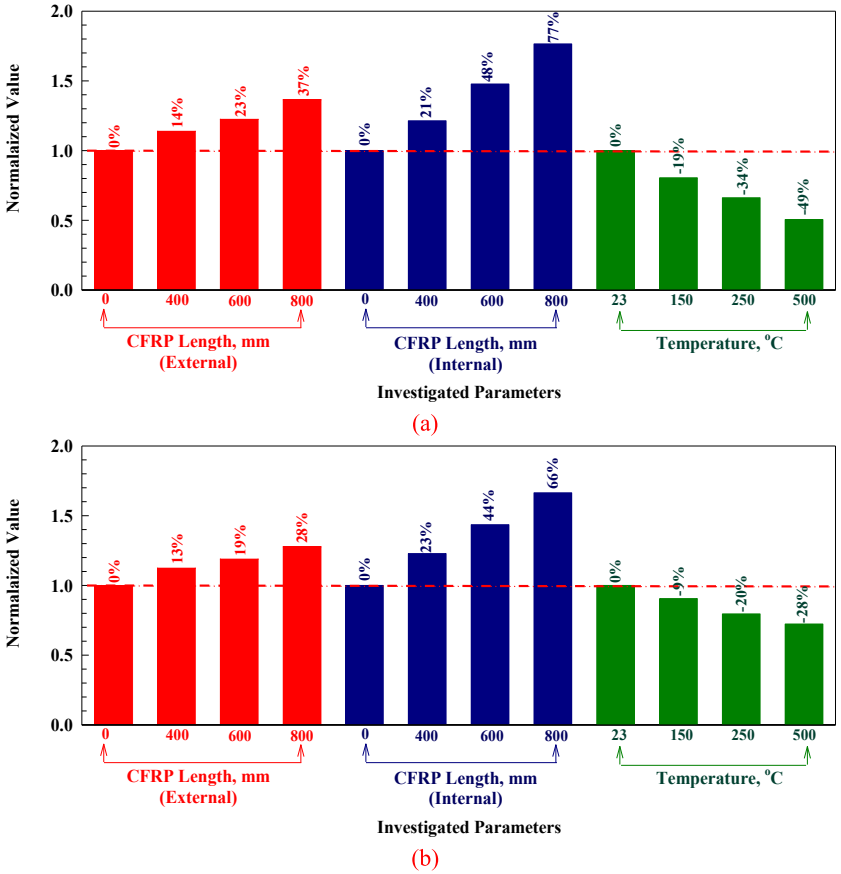

Fig. 12. (a) Ultimate load and (b) ultimate deflection normalization.

findings demonstrated that for every 1% reduction in concrete compressive strength, the average ultimate load was reduced by 0.8%. In contrast, to control beams, the average ultimate deflections were decreased by 9%, 20%, and 28%, respectively, at 150 °C, 250 °C, and 500 °C, equal to 0.55 times the reduction percentage in ultimate loading.

The load vs. CFRP strain values were plotted in Fig. 13 for all tested beams where tensile stresses were developed due to the developed flexural cracks. The load-strain curve is mainly composed of two main parts. The first one is when the resulting stresses are still within the elastic region where the CFRP strain are most-likely neglected, while the second part undergoes a small increase in the

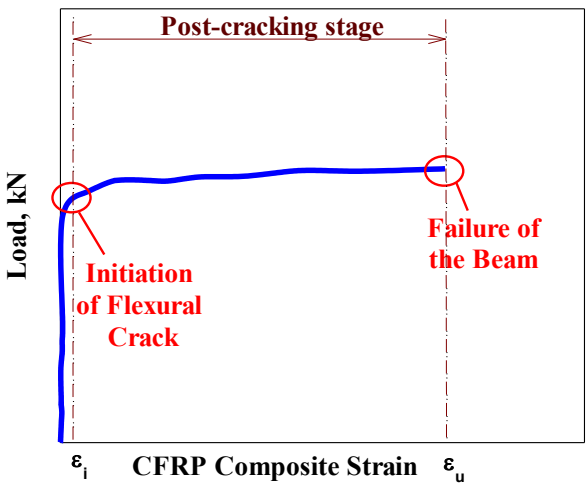

Fig. 13. Typical load versus CFRP strain.

loading values, corresponding to a significant increase in the CFRP strains. However, this increase occurs due to the flexural cracks intensifying within the beam surfaces where the CFRP sheets only provide the beam's resistance. Toumi et al. [50] investigated the influence of residual mechanical strength of concrete when subjected to temperatures (300–700 °C) for an exposure time between one to 9 h. The results indicate that when rising the concrete temperature, the most observable trend was a loss in concrete residual compressive strength.

Moreover, the middle of the CFRP composite generated the highest tensile loads, bridging the midspan flexural cracks, as illustrated in Fig. 11 (a, b), and almost no CFRP strain forms during the pre-cracking stage. Fig. 13 demonstrates how the CFRP strain increased rapidly and gradually until the beam collapsed due to the emergence of flexural cracks in the center of the span, accompanied by steel reinforcement yielding. This indicates that to provide a high-quality strengthening system, CFRP strengthening sheets must be positioned densely close to the midspan of the beam. The findings also provided insight into beams that reached flexural failure prior to the maximum tensile strain capacity of the CFRP sheets, and the failure observed while the CFRP sheet did not experience any stress supported this conclusion. All tested beams showed CFRP strains below the maximum value of 16700 as a percentage of the maximum CFRP strain, as shown in Table 5.

Table 1's analysis reveals that the position of the reinforcement significantly affected the CFRP sheet's effectiveness percentages. For CFRP lengths of (400 mm, 600 mm, and 800 mm), the CFRP/fu (%) percentages were 31%, 36%, and 42%, respectively, with an average value of approximately 36.3%. For CFRP lengths of 400 mm, 600 mm, and 800 mm, employing CFRP composite as internal flexural strengthening had percentages of 41%, 54%, and 72%, with an average value of 55.7%, about 1.53 times that of using CFRP composite as external strengthening. A full composite interaction was demonstrated between the different materials by transmitting tensile forces generated within the internal CFRP composite from the concrete. Also, inner CFRP composites achieved a higher percentage of their maximum capacity; as a result, they are more economical than exterior CFRP used for similar designs. In conclusion, using an internal CFRP sheet to strengthen reinforced concrete beams is a good cost, failure mechanism, and maximum CFRP strain strategy. Kodur and Agrawal [51] studied bond degradation due to the influence of high temperature in RC beams subjected to fire; the study represented that the bond strength in RC beams decreases with the increase in temperature.

The findings show that increased temperature had a negligible effect on the performance of the interior CFRP sheet (in contrast to the influence of reinforcing location). For CFRP lengths of 400 mm, 600 mm, and 800 mm, respectively, the percentage of beams subjected to 150 °C in terms of the maximum strain of the sheet is 34%, 43%, 53%, and 52.2%. Moreover, that is similar to 0.78 of the beam stresses subjected to 23 °C. In addition, the result illustrates that interior CFRP's efficiency was reduced by 22% with a temperature increase of 550% (compared to 23 °C). Furthermore, the percentage of beams exposed to the maximum strain of the CFRP sheet at 250 °C was 25%, 34%, 46.2%, and 44% for CFRP lengths of (400 mm, 600 mm, and 800 mm). That was similar to 0.62 of the stresses on the beam at 23 °C. This suggests that the efficiency of interior CFRP was reduced by 38% due to the 980% temperature elevation (compared to 23 °C). For CFRP lengths of (400 mm, 600 mm, and 800 mm), respectively, the proportion of beams exposed to 500 °C in comparison to the maximum strain of the CFRP sheet was 22%, 30%, and 37%, which was equivalent to 0.53 of the stresses of the beam exposed to 23 °C. This shows that the interior CFRP performance was decreased by 47% due to the 2070% temperature rise (compared to 23 °C).

3.4. Load-deflection curves, stiffness, and toughness

The behavior of each tested beam is shown in Fig. 14 (a, b) in terms of the load-deflection curves, which mainly include a pre-

Table 5
Load deflection behaviour characteristics.

Group	Beam	T, °C	Stiffness, kN/mm	Toughness, kN.mm	DF	SF	PF	STF	TF
1	FB1T23-0-E	23	28.9	1116	2.57	1.18	3.02	1.00	1.00
	FB1T23-400-E		32.6	1452	2.89	1.19	3.43	1.13	1.30
	FB1T23-600-E		34.7	1665	3.06	1.20	3.67	1.20	1.49
	FB1T23-800-E		37.1	1983	3.28	1.25	4.09	1.29	1.78
2	FB2T23-0-I	23	28.9	1116	2.57	1.18	3.02	1.00	1.00
	FB2T23-400-I		34.1	1713	3.33	1.20	4.01	1.18	1.54
	FB2T23-600-I		40.2	2439	4.12	1.25	5.13	1.39	2.19
	FB2T23-800-I		46.2	3446	5.07	1.29	6.56	1.60	3.09
3	FB3T150-0-I	150	22.6	845	2.43	1.17	2.83	1.00	1.00
	FB3T150-400-I		27.0	1119	2.71	1.19	3.23	1.14	1.26
	FB3T150-600-I		32.1	1545	3.03	1.21	3.67	1.35	1.74
	FB3T150-800-I		37.3	2193	3.49	1.28	4.47	1.57	2.47
4	FB4T250-0-I	250	19.6	655	2.29	1.14	2.60	1.00	1.00
	FB4T250-400-I		23.7	859	2.48	1.14	2.84	1.09	1.18
	FB4T250-600-I		28.2	1155	2.74	1.16	3.16	1.30	1.59
	FB4T250-800-I		32.7	1703	3.24	1.23	3.98	1.50	2.34
5	FB5T500-0-I	500	15.6	478	2.21	1.06	2.35	1.00	1.00
	FB5T500-400-I		19.0	629	2.34	1.10	2.58	1.06	1.15
	FB5T500-600-I		22.9	807	2.47	1.12	2.77	1.28	1.47
	FB5T500-800-I		26.6	1023	2.63	1.15	3.03	1.48	1.86

Note: DF: Ductility factor, SF:Strength factor, PF: Performance factor = Ductility factor × Strength factor, TF: Toughness factor, STF: Stiffness factor.

cracking straight line and a post-cracking stage where the slope shifts to characterize the beam's behavior after the onset of cracking was reached. However, stiffness was theoretically calculated as the slope of the linear elastic part in the load-deflection curve [52]. Therefore, it is the ratio between the cracking load and deflection values. Generally, internally and externally strengthened beams exhibited enhanced load-carrying capacities compared to the control ones. Furthermore, figures demonstrated that the efficiency of the beams increased with increasing the bonding area; hence, beams with an 800 mm CFRP sheet length have better performance than those with a 400 mm length. Besides, the CFRP-strengthened beams have improved stiffness, ultimate strength, and ultimate deflection performance, and this further increased under increasing the utilized CFRP length. On the other hand, beams strengthened by a particular length of interior CFRP sheet displayed greater stiffness, maximum strength, and maximum deflection than those strengthened with a similar length of exterior CFRP sheet. However, a hybrid internal strengthening material enhanced the beam's overall behavior [53].

In addition to the maximum load capacity, engineers specializing in structural rehabilitation consider other mechanical characteristics such as energy ductility (toughness) and stiffness. According to Table 5, the beam's stiffness is determined by the slope of its linear elastic portion [52,54], whereas toughness was calculated as the area under the load-deflection curve, including both the elastic and plastic regions [55] as illustrated in equations (2) and (3) where K and T are the stiffness and toughness values, respectively. After

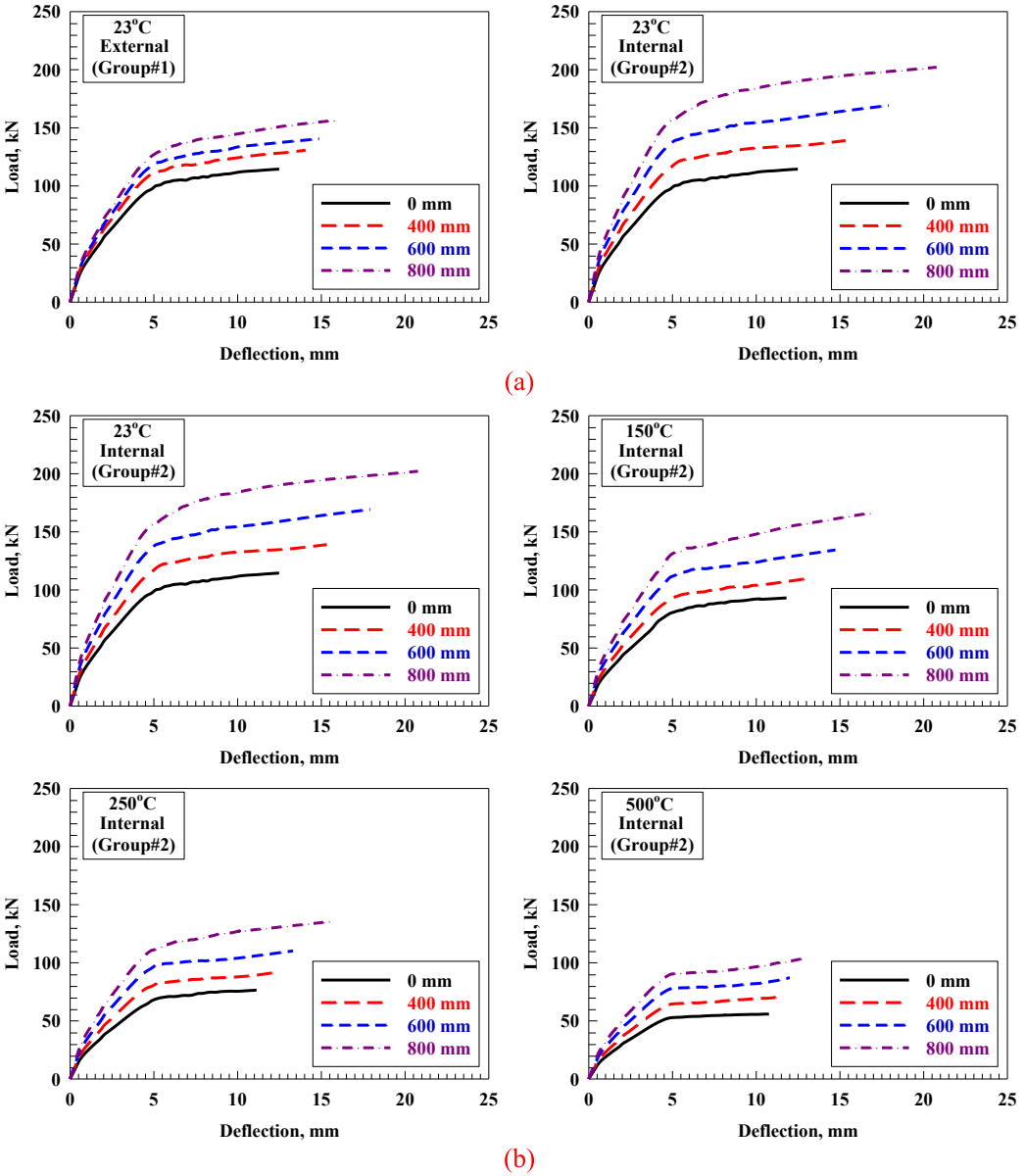

Fig. 14. Load-deflection curves (a) Effect of strengthening location, and (b) Effect of temperature.

being normalized with respect to the control beams, the data were graphically displayed to indicate the difference between stiffness and toughness, as shown in Fig. 15 (a, b). The elastic stiffness of externally strengthened beams was increased by 19%, 33%, 45%, and 55%, respectively, using 1, 2, 3, and 4 CFRP sheets (Fig. 15 (a)). Toughness increased by 26%, 47%, 69%, and 88%, almost 160% of elastic stiffness (Fig. 15 (b)). However, fracture toughness could be calculated for beams at 0.85 times the post-peak load value or at the final reached load, where the two approaches were examined and compared throughout the literature [56–58].

$$k = \frac{P_{cr}}{\Delta_{cr}} \tag{2}$$

$$T = \int_0^{\Delta_u} P du \tag{3}$$

Including 1, 2, 3, and 4 CFRP sheets increased the elasticity of the beams by 21%, 48%, 63%, and 85%, respectively. According to Fig. 15(b), the increases in toughness were 39%, 80%, 115%, and 152%. Comparing internal CFRP sheets to exterior ones increased elastic stiffness and toughness by 155% and 172%, respectively, while interior CFRP sheets resulted in the highest levels of concrete confining and diagonal deformation, which was useful for toughness. CFRP composites limit the propagation of this cracking as they can transmit and bridge stresses through diagonal cracking. As previously discussed, the effectiveness of RC beams under service loading is improved as a result, as seen by enhanced ultimate and cracking loads, along with stiffness and toughness. This also delays the onset of initial flexural cracking. At 150 °C, 250 °C, and 500 °C, the compressive strength of concrete decreased by 9%, 18%, and 55%, whereas stiffness decreased by 8%, 14%, and 25%. However, concrete's elastic stiffness decreased by 0.45% for every 1% loss in compressive strength. The average toughness decrease at 150 °C, 250 °C, and 500 °C is 12%, 21%, and 47%, respectively. The reduction in toughness capability is 1.88 times greater than those observed by the elastic stiffness of the beams.

3.5. Performance evaluation and CFRP profitability index sheet

Load capacity limitations are the ultimate load in intact control RC beams controlled by the material characteristics of its constituents, while the resulting deflection characterizes the serviceability condition. Two major factors were calculated; the first one is related to the beam's strength capability and is known as the Strength Factor (SF), measured as the ultimate strength divided by the strength value corresponding to 0.001 concrete strain where the linear behavior ends. The second major is the Deformability Factor (DF), represented by the deflection ratio at ultimate and 0.001 strain. The two factors were used to calculate the well-known Performance Factor (PF) by multiplying the DF and SF factors and to describe the total effectiveness of the repaired composite beams [59], as shown in equation (4).

$$PF = SF \times DF \tag{4}$$

However, all of the mentioned characteristics are essential for determining whether CFRP composites can increase the overall performance of the strengthened element. Table 4 shows that increasing the number of CFRP sheets for both internal and external strengthening increased performance, stiffness, and toughness values. As a result, reinforced concrete beams' performance, stiffness, and toughness are considerably enhanced by inserting CFRP sheets internally instead of externally. However, as the temperature increased, these elements' impacts are illustrated in Table 5. Peng and Huang [60] reported the alteration in the microstructure of hardened cement paste when subjected to high temperatures. It was noticed that around the 560 °C temperature, the degradation of *C*–S–H started but sharply increased above 600 °C temperature, which this the main reason for the strength loss of concrete when exposed to temperatures above 600 °C.

The effectiveness of the utilized CFRP configuration could be done using more than one approach, such as the cost-effectiveness [57] or profitability index [61] methods. However, the cost of the utilized strengthening approaches could be roughly estimated where the internal strengthening was found to be more cost-effective due to the eliminated cost of the adhesive material. Therefore, results were mainly compared in terms of their profitability indicators which are mainly related to the resulted enhancement in the strength capacity of the heat-damaged RC beams. The profitability index is defined by Shbeeb et al. [61] as the difference in strength values between the strengthened and unstrengthened beams (CFRP strength contribution) divided by the contact area between the CFRP and concrete material surfaces, ensuring that the beams were molded, reinforced, manufactured, and tested under the same circumstances. The profitability index for various reinforcement techniques is displayed in Fig. 16. The profitability indexes decrease as sheet number and temperature increase. The maximum failure load increases as the CFRP bonded area (number of CFRP sheets) increases. This decreases the profitability indices and delays debonding. Based on the quantity used, these findings provide an important criterion for evaluating the effectiveness of using CFRP sheets for interior and external reinforcement.

3.6. Optimization using the linear weighted sum method

The two methods of CFRP strengthening were compared using the linear weighted sum methods [57,62], where three main mechanical characteristics were utilized (loading capacity, ultimate deflection, and toughness). The weighted averages were computed after the P_i values were recorded using the T-test with 95% confidence interval. However, the W values were measured using equation (5).

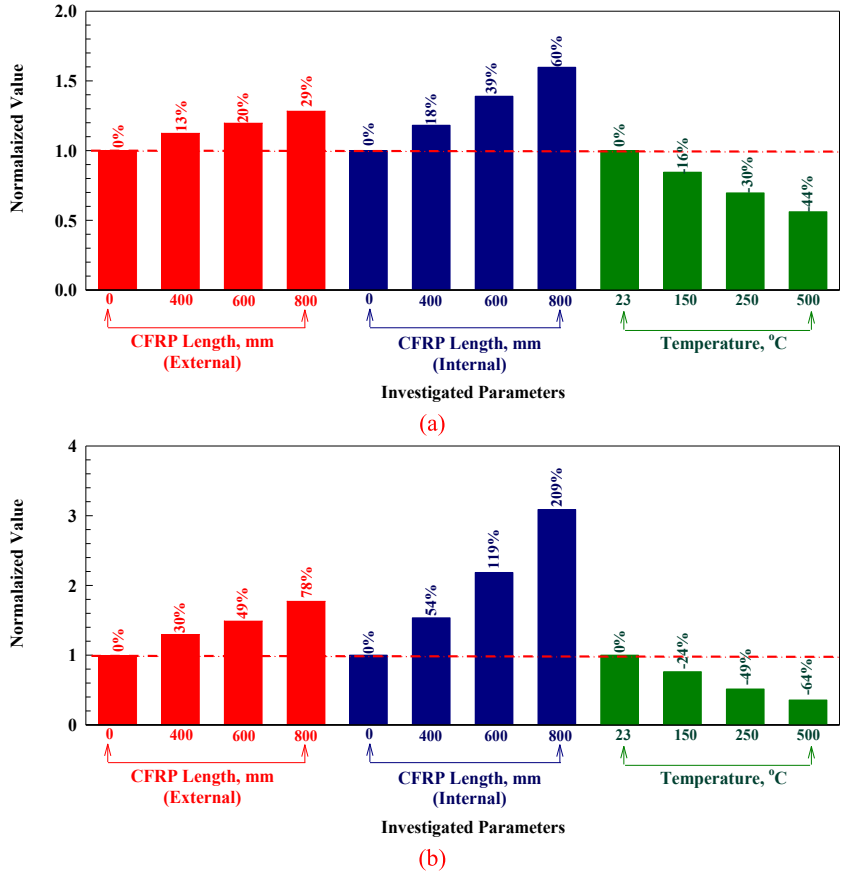

Fig. 15. Characteristic factor normalization (a) Elastic stiffness, and (b) Toughness.

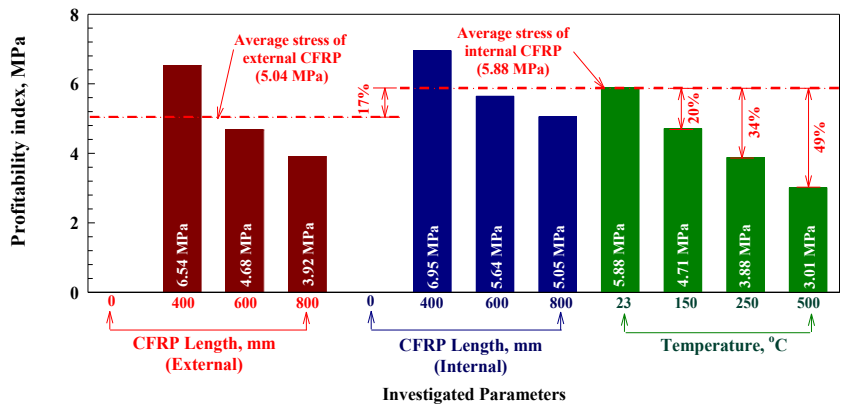

Fig. 16. Profitability index of CFRP strips.

$$W_i = \frac{1 - P_i}{\sum_{i=1}^{n} (1 - P_i)} \tag{5}$$

The optimization test was further done by comparing the external and internal CFRP strengthening unused different sheet lengths at ambient temperatures. However, the results will be the same for the heat-damaged specimens. For ranking and optimizing the strengthened RC beams, the maximum experimentally obtained results were multiplied by the resulted weight of each subcriteria, then the multiplication values for all categories were summed and ranked accordingly. Results are illustrated in Tables 6 and 7, where it has been found that internal strengthening has higher efficiency. In addition, increasing the length of the utilized CFRP sheet enhances the

efficiency of the tested RC specimen, either externally or internally.

It has been demonstrated from the literature that debonding is the major cause of failure in the flexural strengthened RC beams. Different external CFRP configurations were examined by Dong et al. [25] and Nawaz et al. [5], where the ultimate capacity of the tested beams was limited to the CFRP debonding occurrence. Moreover, the effect of CFRP strengthening length was studied by Thomson et al. [63]; where they realized that for external strengthening, it is required a certain length of the strengthening material for the ultimate capacity of the RC beam to be increased and known as the development length, but still the dominant behavior was the debonding of the strengthening material. Therefore, the author proposed the internal strengthening technique as a new technique for eliminating the adhesive bonding issues, and it proved to be effective in terms of cost (due to eliminated usage of adhesive material) and efficiency, besides increasing its effectiveness by increasing the length of the internally applied CFRP sheet which confirmed to the result of the linear weight sum method.

3.7. Guidelines on the effect of heat damage on the load-carrying capacity

A visual map guideline was provided in Fig. 17, linking the combined effect of increasing the exposed temperature and the resulting damage levels where the concrete compressive strength was highly reduced. The contribution of the main constitutes was considered, including the CFRP sheets (P_F), main flexural steel reinforcement (P_u), and concrete material (P_c). However, the plotted damage could be divided into three main regions based on their damage extent as given by the ACI440-17 code [6]. The environmental condition was the main criterion for the divided regions. The first one is for the interior exposure with a 5%–15% damage level, the second represents the exterior exposure with a damage level that varies between 15% and 50%, and the last one is for the aggressive exposure with 50%–100% damage. Therefore, the proposed guideline was divided accordingly. Observing Fig. 17 reveals that the contribution of the three plotted components (concrete, steel, and CFRP) varies under high temperatures, having the same exponential trends but with different rates. However, differences appear after a temperature level of approximately 200 ° C, the three curves deviate from each other. This could be interpreted by the reduction in the material's internal structure, besides the reduction in their bond at the interface with other constituents, such as the CFRP-concrete interface.

The guideline could be utilized to directly predict the reduction factor for the concrete, steel, and CFRP material under elevated temperatures ($P_c, P_u,$ and P_F) with a wide range between 0 and 500 ° C. The three divided regions (based on the ACI440 code) are located between $(0-200)^{\circ}$ C, $(200-340)^{\circ}$ C, and $(>340)^{\circ}$ C for the interior, exterior, and aggressive exposures. Results were compatible with those predicted by the ACI440 code, where concrete undergoes high damage after exposure to temperature levels beyond 300 ° C. The proposed guideline in Fig. 17 might be utilized and highly assist engineers in designing and rehabilitation RC beams with CFRP composites after being subjected to elevated temperatures.

4. Conclusion

The findings of this study could be highly utilized by engineers and assist in designing and rehabilitating RC beams using CFRP composites using a feasible and efficient technique eliminating the unfavorable debonding issue. Based on the previous results and discussion, the following could be concluded:

1) For flexural reinforcement of RC beams, installing an internal sheet of CFRP is uncomplicated and does not require any adhesive or anchoring material. Also, it is simple to cut and place in the desired area, but attention is needed when pouring the concrete to avoid damaging the CFRP sheets.
2) The structural performance is significantly enhanced upon strengthening by either external or internal CFRP strips, where the beam's ultimate capacity, ultimate deflection, stiffness, and toughness were all increased compared to un-strengthened ones. However, the enhancement percentages are twice as much for internal strengthening as the external one.
3) The increased temperature had a negligible effect on the performance of the interior CFRP sheet.
4) The enhancement in the ultimate deflection was 2.21 times the provided in external CFRP strengthening compared to 1.97 for the ultimate load.

Table 6
Weighted average and maximum values for the RC beams mechanical properties.

Group	Beam	Pu, kN		Δ_u, mm		Toughness, kN.mm	
		Weight	Max value	Weight	Max value	Weight	Max value
1	FB1T23-0-E	0.139272	114.5	0.144809	12.5	0.141504	1116
	FB1T23-400-E	0.127363	130.7	0.131648	14.1	0.131070	1452
	FB1T23-600-E	0.096929	140.5	0.105077	14.9	0.108635	1665
	FB1T23-800-E	0.116833	156.6	0.100301	16.0	0.094571	1983
2	FB2T23-0-I	0.139268	114.5	0.144809	12.5	0.141504	1116
	FB2T23-400-I	0.103356	139.0	0.084372	15.3	0.100968	1713
	FB2T23-600-I	0.136395	169.2	0.142880	17.9	0.138214	2439
	FB2T23-800-I	0.140583	202.1	0.146106	20.8	0.143534	3446

Table 7
Optimization results and ranking.

Group	Beam	Outcome	Ranking
1	FB1T23-0-E	175.6752	8
	FB1T23-400-E	188.3021	5
	FB1T23-600-E	196.0614	6
	FB1T23-800-E	207.4352	4
2	FB2T23-0-I	193.2156	7
	FB2T23-400-I	208.8162	3
	FB2T23-600-I	362.7395	2
	FB2T23-800-I	526.069	1

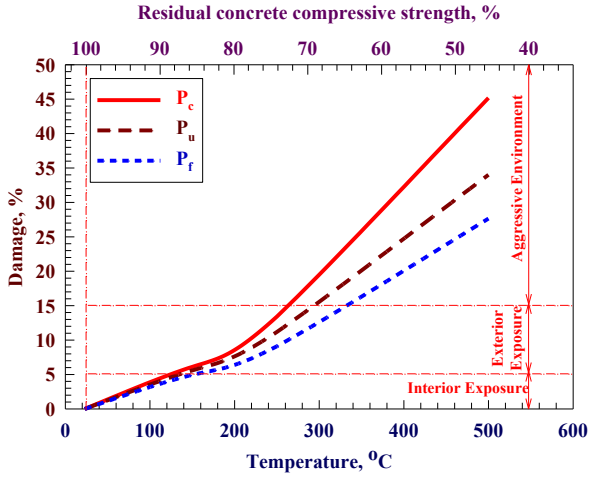

Fig. 17. Ultimate, failure, CFRP load versus heat damage.

5) Internally reinforced CFRP beams might be subjected to various cracking at multiple locations due to the considerable CFRP development length provided within the RC beam where CFRP sheet rupture possibility is increased. In contrast, beams strengthened with external CFRP failed in bending and delamination at the end strip location.
6) Strengthening heat-damaged RC beams with an external or internal CFRP strip significantly improves their behavior. Besides, increasing the length of the utilized strips increases the resulting enhancement under all temperatures.
7) The position of the reinforcement significantly affected the CFRP sheet's effectiveness percentages, where internal strengthening exhibits CFRP strain values 1.53 times higher than those of the external position.
8) Concrete's elastic stiffness decreased by 0.45% for every 1% loss in compressive strength, and the reduction in toughness capability is 1.88 times greater than those observed by the elastic stiffness of the beams. The average toughness decrease at 150 °C, 250 °C, and 500 °C is 12%, 21%, and 47%, respectively.
9) Beams strengthened by a particular length of interior CFRP sheet displayed greater stiffness, maximum strength, and maximum deflection than those strengthened with a similar length of exterior CFRP sheet.
10) The efficiency of the new technique has been demonstrated using the linear weighted sum method after being compared with other CFRP configurations and having the highest ranking.

5. Limitations

Despite the highest efficiency of the newly proposed strengthening technique compared to the conventionally utilized external CFRP strengthening, its main limitations affect its field of application, mainly applied before the concrete casting stage. Therefore, high attention is required for the strengthening material to remain in its position. Besides, the internal strengthening technique is limited in its use for RC members before being casted or repaired after the concrete cover is replaced.

Author contribution statement

Rajai Z. Al-Rousan: Conceived and designed the experiments; Performed the experiments; Analyzed and interpreted the data; Contributed reagents, materials, analysis tools or data; Wrote the paper. </p>

Data availability statement

Data will be made available on request.

Declaration of competing interest

The authors declare the following financial interests/personal relationships which may be considered as potential competing interests:Rajai Al Rousan reports article publishing charges was provided by Jordan University of Science and Technology. Rajai Al Rousan reports a relationship with Jordan University of Science and Technology that includes: employment.

Acknowledgments

The author gratefully acknowledges the financial support from the Deanship of Scientific Research at Jordan University of Science and Technology under Grant number 2022/340.

References

[1] N.I. Rahim, B.S. Mohammed, A. Al-Fakih, M.M.A. Wahab, M.S. Liew, A. Anwar, Y.H.M. Amran, Strengthening the structural behavior of web openings in RC deep beam using CFRP, Materials 13 (12) (2020) 2804, https://doi.org/10.3390/ma13122804.
[2] R.Z. Al-Rousan, B.R. Alnemrawi, Punching shear code provisions examination against the creation of an opening in existed RC flat slab of various sizes and locations, Structures 49 (2023) 875–888, https://doi.org/10.1016/j.istruc.2023.02.007.
[3] M.M.A. Kadhim, A.H. Adheem, A.R. Jawdhari, Nonlinear finite element modelling and parametric analysis of shear strengthening RC T-beams with NSM CFRP technique, Int. J. Civ. Eng. 17 (8) (2019) 1295–1306, https://doi.org/10.1007/s40999-018-0387-8.
[4] R.A. Hawileh, J.A. Abdalla, M.Z. Naser, Modeling the shear strength of concrete beams reinforced with CFRP bars under unsymmetrical loading, Mech. Adv. Mater. Struct. 26 (15) (2019) 1290–1297, https://doi.org/10.1080/15376494.2018.1432803.
[5] W. Nawaz, M. Elchalakani, A. Karrech, S. Yehia, B. Yang, O. Youssf, Flexural behavior of all lightweight reinforced concrete beams externally strengthened with CFRP sheets, Construct. Build. Mater. 327 (2022), 126966, https://doi.org/10.1016/j.conbuildmat.2022.126966.
[6] ACI440 Guide for the Design and Construction of Externally Bonded FRP Systems for Strengthening Concrete Structures, American Concrete Institute, 2017.
[7] M.A. Al-Osta, K.M. Kharma, S. Ahmad, M. Maslehuddin, M. Al-Huri, H. Khalid, Strategies for strengthening of corroded reinforced concrete beams using CFRP laminates and UHPC jacketing, Struct. Concr. 24 (1) (2023) 1546–1571, https://doi.org/10.1002/suco.202200211.
[8] C. Barris, P. Sala, J. Gómez, L. Torres, Flexural behaviour of FRP reinforced concrete beams strengthened with NSM CFRP strips, Compos. Struct. 241 (2020), 112059, https://doi.org/10.1016/j.compstruct.2020.112059.
[9] R.Z. Al-Rousan, M.F. AL-Tahat, Consequence of surface preparation techniques on the bond behavior between concrete and CFRP composites, Construct. Build. Mater. 212 (2019) 362–374, https://doi.org/10.1016/j.conbuildmat.2019.03.299.
[10] M.A. Alhassan, R.Z. Al Rousan, E.A. Al Shuqari, Bond-slip behavior between fiber reinforced concrete and CFRP composites, Ain Shams Eng. J. 10 (2) (2019) 359–367, https://doi.org/10.1016/j.asej.2019.03.001.
[11] R. Al-Rousan, R. Haddad, A. Al-Halboni, Bond–slip behaviour between self-compacting concrete and carbon-fibre-reinforced polymer sheets, Mag. Concr. Res. 67 (2) (2015) 89–103, https://doi.org/10.1680/macr.14.00150.
[12] H.L. Lye, B.S. Mohammed, M.S. Liew, M.M.A. Wahab, A. Al-Fakih, Bond behaviour of CFRP-strengthened ECC using response surface methodology (RSM), Case Stud. Constr. Mater. 12 (2020), e00327, https://doi.org/10.1016/j.cscm.2019.e00327.
[13] A. Al-Fakih, M. Hisbany Mohd Hashim, R. Alyousef, A. Mutafi, S. Hussein Abo Sabah, T. Tafsirojjaman, Cracking behavior of sea sand RC beam bonded externally with CFRP plate, Structures 33 (2021) 1578–1589, https://doi.org/10.1016/j.istruc.2021.05.042.
[14] A.O. Sojobi, K.M. Liew, Multi-objective optimization of high performance concrete columns under compressive loading with potential applications for sustainable earthquake-resilient structures and infrastructures, Compos. Struct. 315 (2023), 117007, https://doi.org/10.1016/j.compstruct.2023.117007.
[15] R.K. Manikandan, K. Shunmugapriya, J. Arunprasad, S. Sugumar, D. Manikandan, Retrofitting of reinforced concrete beams using CFRP with various adhesive, Mater. Today: Proc. 68 (2022) 1635–1640, https://doi.org/10.1016/j.matpr.2022.07.448.
[16] T.H. Almusallam, Y.A. Al-Salloum, Durability of GFRP rebars in concrete beams under sustained loads at severe environments, J. Compos. Mater. 40 (7) (2006) 623–637, https://doi.org/10.1177/0021998305055275.
[17] O. Chaallal, M.J. Nollet, D. Perraton, Shear strengthening of RC beams by externally bonded side CFRP strips, J. Compos. Construct. 2 (2) (1998) 111–113, 10.1061/ASCE)1090-0268(1998)2:2(111.
[18] N. Pannirselvam, V. Nagaradjane, K. Chandramouli, Strength behaviour of fibre reinforced polymer strengthened beam, J. Eng. Appl. Sci. 4 (9) (2009) 34–39.
[19] A.S. Saadoon, Effect of CFRP strips orientation on performance of strengthened deep beams, Al-Qadisiyah Journal for Engineering Sciences 12 (3) (2019) 172–177, https://doi.org/10.30772/qjes.v12i3.614.
[20] A.H. Al-Abdwais, R.S. Al-Mahaidi, Evaluation of high temperature endurance of RC beams retrofitted with NSM technique using CFRP composites and modified cement-based adhesive, Eng. Struct. 264 (2022), 114445, https://doi.org/10.1016/j.engstruct.2022.114445.
[21] A. Khalifa, A. Nanni, Improving shear capacity of existing RC T-section beams using CFRP composites, Cement Concr. Compos. 22 (3) (2000) 165–174, https://doi.org/10.1016/S0958-9465(99)00051-7.
[22] C. Deniaud, J.R. Cheng, Shear behavior of reinforced concrete T-beams with externally bonded fiber-reinforced polymer sheets, Structural journal 98 (3) (2001) 386–394.
[23] A. Bousselham, O. Chaallal, Mechanisms of shear resistance of concrete beams strengthened in shear with externally bonded FRP, J. Compos. Construct. 12 (5) (2008) 499–512, https://doi.org/10.1061/(ASCE)1090-0268, 2008)12:5(499.
[24] A. ACI, Building Code Requirements for Structural Concrete and Commentary, 2014.
[25] J. Dong, Q. Wang, Z. Guan, Structural behaviour of RC beams with external flexural and flexural–shear strengthening by FRP sheets, Compos. B Eng. 44 (1) (2013) 604–612, https://doi.org/10.1016/j.compositesb.2012.02.018.
[26] V. Kodur, A. Agrawal, An approach for evaluating residual capacity of reinforced concrete beams exposed to fire, Eng. Struct. 110 (2016) 293–306, https://doi.org/10.1016/j.engstruct.2015.11.047.
[27] A. Al-Ostaz, M. Irshidat, B. Tenkhoff, P.S. Ponnapalli, Deterioration of bond integrity between repair material and concrete due to thermal and mechanical incompatibilities, J. Mater. Civ. Eng. 22 (2) (2010) 136–144, https://doi.org/10.1061/(ASCE)0899-1561, 2010)22:2(136.
[28] R.Z. Al-Rousan, B.R. Alnemrawi, Cyclic behavior of CFRP confined circular CFST damaged by alkali-silica reaction, Int. J. Civ. Eng. 21 (7) (2023) 1–22, https://doi.org/10.1007/s40999-023-00820-w.
[29] R.Z. Alrousan, B.R. Alnemrawi, The behavior of alkali-silica reaction-damaged full-scale concrete bridge deck slabs reinforced with CFRP bars, Results in Engineering 16 (2022), https://doi.org/10.1016/j.rineng.2022.100651.

[30] V.J. Ferrari, J.B. de Hanai, R.A. de Souza, Flexural strengthening of reinforcement concrete beams using high performance fiber reinforcement cement-based composite (HPFRCC) and carbon fiber reinforced polymers (CFRP), Construct. Build. Mater. 48 (2013) 485–498, https://doi.org/10.1016/j.conbuildmat.2013.07.026.
[31] N. Attari, S. Amziane, M. Chemrouk, Flexural strengthening of concrete beams using CFRP, GFRP and hybrid FRP sheets, Construct. Build. Mater. 37 (2012) 746–757, https://doi.org/10.1016/j.conbuildmat.2012.07.052.
[32] I.F. Kara, A.F. Ashour, M.A. Köroğlu, Flexural behavior of hybrid FRP/steel reinforced concrete beams, Compos. Struct. 129 (2015) 111–121, https://doi.org/10.1016/j.compstruct.2015.03.073.
[33] A. Dem'Yanov, The modeling method of discrete cracks in reinforced concrete under the torsion with bending, Magazine of Civil Engineering 5 (81) (2018) 160–173, https://doi.org/10.18720/MCE.81.16.
[34] R. Al-Rousan, A. Ababneh, M. Alhassan, Hybrid CFRP-steel for enhancing the flexural behavior of reinforced concrete beams, Journal of King Saud University-Engineering Sciences 33 (7) (2021) 459–470, https://doi.org/10.1016/j.jksues.2020.06.004.
[35] W. Wang, H. Pan, Y. Shi, Y. Pan, W. Yang, K. Liew, L. Song, Y. Hu, Fabrication of LDH nanosheets on β-FeOOH rods and applications for improving the fire safety of epoxy resin, Compos. Appl. Sci. Manuf. 80 (2016) 259–269, https://doi.org/10.1016/j.compositesa.2015.10.031.
[36] W. Wang, Y. Kan, J. Liu, K.M. Liew, L. Liu, Y. Hu, Self-assembly of zinc hydroxystannate on amorphous hydrous TiO2 solid sphere for enhancing fire safety of epoxy resin, J. Hazard Mater. 340 (2017) 263–271, https://doi.org/10.1016/j.jhazmat.2017.06.068.
[37] Committee A Building Code Requirements for Structural Concrete (ACI 318-08) and Commentary, American Concrete Institute, 2019.
[38] C. Astm, 230/C230-08 Standard Specification for Flow Table for Use in Test of Hydraulic Cement, vol. 4, Annual Book of ASTM Standards, 2008.
[39] ASTM ACJABoAS, 579 standard test methods for compressive strength of chemical-resistant mortars, Grouts, Monolithic Surfacings, and Polymer Concretes 4 (2018).
[40] ASTM, Strength of Cylindrical Concrete Specimens, ASTM International West, Conshohocken, PA, 2017. ASTM C496/C496M-17, Standard Test Method for Splitting Tensile.
[41] A. Std, Annual Book of ASTM Standards, 1989.
[42] M.P. Turunen, P. Marjamäki, M. Paajanen, J. Lahtinen, J.K.J.M.R. Kivilahti, Pull-off test in the assessment of adhesion at printed wiring board metallisation/epoxy interface 44 (6) (2004) 993–1007.
[43] ASTM, Standard Test Method for Tensile Strength of Concrete Surfaces and the Bond Strength or Tensile Strength of Concrete Repair and Overlay Materials by Direct Tension (Pull-off Method), West Conshohocken PA, 2004.
[44] M. Saafi, Effect of fire on FRP reinforced concrete members, Compos. Struct. 58 (1) (2002) 11–20, https://doi.org/10.1016/S0263-8223(02)00045-4.
[45] B. Standard, Eurocode 2: Design of Concrete Structures—, vol. 1, 2004.
[46] R.H. Haddad, R. Al-Rousan, L. Ghanma, Z. Nimri, Modifying CFRP–concrete bond characteristics from pull-out testing, Mag. Concr. Res. 67 (13) (2015) 707–717, https://doi.org/10.1680/macr.14.00271.
[47] M.A. Alhassan, R.Z. Al-Rousan, A.M. Abu-Elhija, Anchoring holes configured to enhance the bond-slip behavior between CFRP composites and concrete, Construct. Build. Mater. 250 (2020), 118905, https://doi.org/10.1016/j.conbuildmat.2020.118905.
[48] H. Jafarzadeh, M. Nematzadeh, Flexural strengthening of fire-damaged GFRP-reinforced concrete beams using CFRP sheet: experimental and analytical study, Compos. Struct. 288 (2022), 115378, https://doi.org/10.1016/j.compstruct.2022.115378.
[49] Y. Al Rjoub, A. Obaidat, A. Ashteyat, K. Alshboul, Experimental and analytical investigation of using externally bonded, hybrid, fiber-reinforced polymers to repair and strengthen heated, damaged RC beams in flexure, J. Struct. Fire Eng. 13 (3) (2022) 391–417, https://doi.org/10.1108/JSFE-09-2021-0059.
[50] B. Toumi, M. Resheidat, Z. Guemmadi, H. Chabil, Coupled effect of high temperature and heating time on the residual strength of normal and high-strength concretes, Jordan Journal of Civil Engineering 3 (4) (2009) 322–330.
[51] V. Kodur, A. Agrawal, Effect of temperature induced bond degradation on fire response of reinforced concrete beams, Eng. Struct. 142 (2017) 98–109, https://doi.org/10.1016/j.engstruct.2017.03.022.
[52] Z. Sun, Y. Yang, W. Qin, S. Ren, G. Wu, Experimental study on flexural behavior of concrete beams reinforced by steel-fiber reinforced polymer composite bars, J. Reinforc. Plast. Compos. 31 (24) (2012) 1737–1745, https://doi.org/10.1016/j.jobe.2021.103087.
[53] L.J. Li, S. Fang, B. Fu, H.D. Chen, M.S. Geng, Behavior of hybrid FRP-concrete-steel multitube hollow columns under axial compression, Construct. Build. Mater. 253 (2020), 119159, https://doi.org/10.1016/j.conbuildmat.2020.119159.
[54] R.Z. Al-Rousan, B.R. Alnemrawi, Prediction of interface shear strength of heat damaged shear-keys using nonlinear finite element analysis, Journal of Applied and Computational Mechanics (2023), https://doi.org/10.22055/jacm.2023.42998.4000.
[55] Y. Ding, Z. You, S. Jalali, Hybrid fiber influence on strength and toughness of RC beams, Compos. Struct. 92 (9) (2010) 2083–2089, https://doi.org/10.1016/j.compstruct.2009.10.016.
[56] L.W. Zhang, A.O. Sojobi, K.M. Liew, Sustainable CFRP-reinforced recycled concrete for cleaner eco-friendly construction, J. Clean. Prod. 233 (2019) 56–75, https://doi.org/10.1016/j.jclepro.2019.06.025.
[57] A.O. Sojobi, K.M. Liew, Flexural behaviour and efficiency of CFRP-laminate reinforced recycled concrete beams: optimization using linear weighted sum method, Compos. Struct. 260 (2021), 113259, https://doi.org/10.1016/j.compstruct.2020.113259.
[58] A.O. Sojobi, K.M. Liew, Multi-objective optimization of high performance bio-inspired prefabricated composites for sustainable and resilient construction, Compos. Struct. 279 (2022), 114732, https://doi.org/10.1016/j.compstruct.2021.114732.
[59] G. Spadea, F. Bencardino, F. Sorrenti, R.N. Swamy, Structural effectiveness of FRP materials in strengthening RC beams, Eng. Struct. 99 (2015) 631–641, https://doi.org/10.1016/j.engstruct.2015.05.021.
[60] G.-F. Peng, Z.-S. Huang, Change in microstructure of hardened cement paste subjected to elevated temperatures, Construct. Build. Mater. 22 (4) (2008) 593–599, https://doi.org/10.1016/j.conbuildmat.2006.11.002.
[61] N.I. Shbeeb, R. Al-Rousan, M.A. Issa, H. Al-Salman, Impact of bonded carbon fibre composite on the shear strength of reinforced concrete beams, Proceedings of the Institution of Civil Engineers–Structures and Buildings 171 (5) (2018) 364–379, https://doi.org/10.1680/jstbu.16.00145.
[62] A.O. Sojobi, D. Xuan, L. Li, S. Liu, C.S. Poon, Optimization of gas-solid carbonation conditions of recycled aggregates using a linear weighted sum method, Developments in the Built Environment 7 (2021), 100053, https://doi.org/10.1016/j.dibe.2021.100053.
[63] H. Thomsen, E. Spacone, S. Limkatanyu, G. Camata, Failure mode analyses of reinforced concrete beams strengthened in flexure with externally bonded fiber-reinforced polymers, J. Compos. Construct. 8 (2) (2004) 123–131, 10.1061/ASCE)1090-0268(2004)8:2(123.